Impact of enhanced ozone deposition and halogen chemistry on tropospheric ozone over the Northern Hemisphere

Golam Sarwar[1,*], Brett Gantt[1], Donna Schwede[1], Kristen Foley[1], Rohit Mathur[1], Alfonso Saiz-Lopez[2]

[1] National Exposure Research Laboratory, Environmental Protection Agency, RTP, North Carolina, USA
[2] Atmospheric Chemistry and Climate Group, Institute of Physical Chemistry Rocasolano, CSIC, Madrid, Spain

*Corresponding author: Golam Sarwar, US EPA, 109 T.W. Alexander Drive, Research Triangle Park, NC 27711, USA; Tel.: 919-541-2669; fax: 919-541-1379; e-*mail*: sarwar.golam@epa.gov

TOC ART

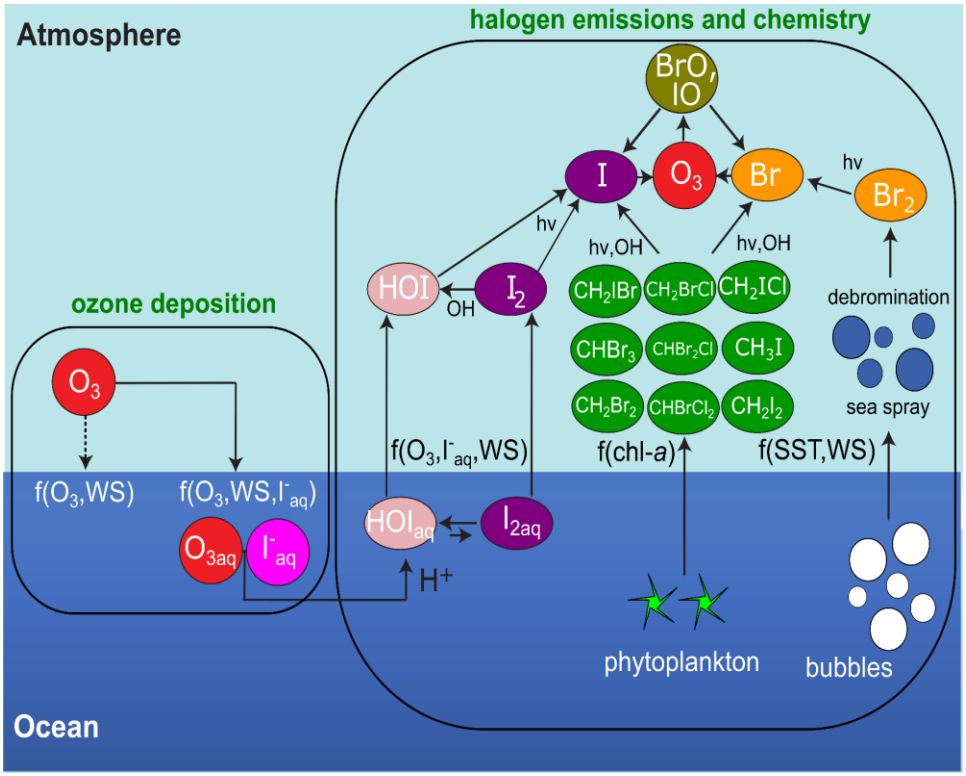
Atmosphere
halogen emissions and chemistry
BrO, IO
I
O3
Br
hv
Br2
hv
hv,OH
hv,OH
HOI
OH
I2
CH2IBr
CH2BrCl
CH2ICl
debromination
ozone deposition
CHBr3
CHBr2Cl
CH3I
O3
CH2Br2
CHBrCl2
CH2I2
sea spray
f(O3,I-aq,WS)
f(chl-a)
f(SST,WS)
f(O3,WS)
f(O3,WS,I-aq)
HOIaq
I2aq
O3aq
I-aq
H+
phytoplankton
bubbles
Ocean

ABSTRACT

Fate of ozone in marine environments has been receiving increased attention due to the tightening of ambient air quality standards. The role of deposition and halogen chemistry is examined through incorporation of an enhanced ozone deposition algorithm and inclusion of halogen chemistry in a comprehensive atmospheric modeling system. The enhanced ozone deposition treatment accounts for the interaction of iodide in seawater with ozone and increases deposition velocities by an order of magnitude. Halogen chemistry includes detailed chemical reactions of organic and inorganic bromine and iodine species. Two different simulations are completed with the halogen chemistry: without and with photochemical reactions of higher iodine oxides. Enhanced deposition reduces mean summertime surface ozone by ~3% over marine regions in the Northern Hemisphere. Halogen chemistry without the photochemical reactions of higher iodine oxides reduces ozone by ~15% while simulations with the photochemical reactions of higher iodine oxides indicate ozone reductions of ~48%. Model without these processes over-predicts ozone compared to observations while the inclusion these processes improves predictions. The inclusion of photochemical reactions for higher iodine oxides leads to ozone predictions that are lower than observations, underscoring the need for further refinement of the halogen emissions and chemistry scheme in the model.

Keywords: ozone, ozone deposition, halogen, iodine, bromine

1.0 INTRODUCTION

Ozone (O_3) has been linked to adverse effects on human health[1] and ecosystems.[2] To mitigate these effects, air quality standards have been periodically revised which has led to the tightening of ambient air quality standards for O_3. The tightened ambient air quality standards make the determination of background O_3 levels more important. Background levels of O_3 are affected by mixing ratios over the ocean, which are influenced greatly by the chemicals present in the sea surface microlayer. These chemical compounds can be emitted to the atmosphere and affect atmospheric chemistry and can also serve as a chemical sink to enhance deposition to the seawater surface. Studies have suggested that O_3 deposition over seawater is highly variable due to variations in atmospheric O_3 mixing ratio and deposition velocity (flux/mixing ratio), with reported deposition velocities ranging from 0.009 to ~0.27 cm s^{-1}.[3-4] The deposition velocity over seawater is dependent on a number of factors including the atmospheric turbulence and the chemical composition of the seawater. While several compounds in seawater can interact with O_3[5-7] and the presence of other compounds can affect such interactions[8], there is still much uncertainty in modeling these interactions. Considerably more consensus has been reached on the interaction between O_3 and iodide in the seawater. Developing reliable spatial distributions of iodide concentrations in seawater is key and concentrations have been estimated using various proxies, including chlorophyll-*a* (chl-*a*)[9], nitrate[10], and sea surface temperature (SST)[10,11]. Several models of the enhanced deposition of O_3 over sea water have been proposed ranging from complex approaches such as that of Fairall et al.[12] to more simple approaches such as that of Chang et al[5]. Oh et al.[9] employed the simple approach of Chang et al.[5] and linked O_3 dry deposition velocities to satellite-derived chl-*a* concentrations and reported a maximum surface O_3 decrease of 2.5 ppbv offshore of Galveston, Texas. While the Oh et al.[9] study suggests

enhanced deposition of O_3 over sea-water can affect atmospheric O_3 in areas of the Gulf of Mexico, little is known about its importance in other coastal areas.

Although several studies have postulated that bromine and iodine emitted from the ocean impact atmospheric chemistry[13-15], recent measurements of speciated halogen species with advanced instrumentation have confirmed the presence of an oceanic halogen emission source[16-20]. The sea-air flux and associated chemistry of bromine- and iodine-containing compounds affects new particle formation, mercury cycling, oxidative capacity, and O_3 mixing ratio of the marine atmosphere.[17, 21-23] These halogen species undergo photolysis and react with oxidants to release iodine or bromine, which can then catalytically react with O_3 to reduce its levels in the marine atmosphere. With the increasing focus on background O_3 levels, marine halogen sources/chemistry have been the subject of several recent laboratory, field, and modeling studies.[24-38] Laboratory studies report that the reactions of O_3 and marine aerosols can release halogens[24, 27] and water surface properties can also affect these reactions[26, 28]. While the reaction of O_3 with bromide is generally low[39], some studies reveal the possibility of a surface-mediated reaction that can enhance the reaction rate leading to the loss of O_3 and release of gaseous bromine[24, 25, 28].

In recent years, several modeling studies have attempted to represent marine halogen emission sources and atmospheric chemistry with increasing levels of complexity. Beginning with the one dimensional modeling work of halogen chemistry in the atmosphere[29-30], various marine emission sources such as halocarbons[31-32], sea spray aerosol (SSA) bromine[33], and iodine/hypoiodous acid[11] and chemical reactions such as photolysis of higher iodine oxides[34]

have been implemented into global chemical transport models. Saiz-Lopez et al.[35] found that tropospheric O_3 loss due to marine halogen emissions can have a climatically-relevant radiative impact while Parrella et al.[36] postulate that the inclusion of bromine chemistry improves model prediction of pre-industrial O_3 observations and leads to differential mercury lifetimes in pre-industrial and present-day conditions. Long et al.[37] report that bromine activated from SSA reduces marine boundary layer O_3 by >20% over most of the tropics and >75% over the Southern Ocean. Despite the demonstrated impact of enhanced deposition of O_3 over seawater and marine halogen emissions/chemistry on O_3 mixing ratios, these processes are currently not accounted for in most regional air quality models. The reaction between O_3 and dissolved iodide in seawater not only decreases atmospheric O_3 but also generates halogen emissions that activate the atmospheric chemistry of reactive halogens. The loss of atmospheric O_3 due to the reaction of O_3 and dissolved iodide in seawater is modeled using enhanced deposition velocity. In this study, we quantify the impact of enhanced O_3 deposition and marine halogen emissions and chemistry on tropospheric O_3 mixing ratios over the Northern Hemisphere.

2.0 **METHODOLOGY**

2.1 Model description

The Community Multiscale Air Quality (CMAQ) modeling system is a comprehensive regional air quality model accounting for interactions among major atmospheric processes.[40] Many studies have employed the regional CMAQ model and demonstrated its skill in simulating ambient pollutants.[41-44] Mathur et al.[45-46] recently extended the model capabilities for applications to the Northern Hemisphere. Sarwar et al.[47] applied the hemispheric CMAQ model for examining the impacts of heterogeneous nitryl chloride chemistry in the Northern Hemisphere

while Xing et al.[48] used the model for evaluating air quality trends. Here, we employ the on-line hemispheric CMAQ model using a horizontal resolution of 108-km and 44 vertical layers.[48] The CB05TUCl chemical mechanism[42] which integrates chlorine chemistry with the Carbon Bond mechanism was used. Emissions inputs are described in Sarwar et al.[47] and meteorological fields are detailed in Xing et al.[48]. In the following sections, we describe the model implementation of enhanced O_3 deposition (section 2.2), halogen chemistry (section 2.3), and halogen emissions (section 2.4).

2.2 Deposition of species

CMAQ accounts for both the dry and wet deposition of model species, and these treatments have been described in Byun et al.[40] These deposition approaches have been updated to include the necessary parameters for modeling the loss of bromine and iodine species (section 2.3). Here we focus on updates to the deposition of O_3.

The deposition velocity (v_d) for gas species is parameterized in CMAQ using the familiar resistance analogy[49]:

$$v_d = (R_a + R_b + R_s)^{-1} \quad (1)$$

where the aerodynamic resistance (R_a) accounts for atmospheric turbulence, the boundary layer resistance (R_b) represents diffusion across the quasi-laminar near-surface layer, and the surface resistance (R_s) accounts for the uptake by the surface. In CMAQ, the R_s for water surfaces is calculated as[12, 50]:

$$R_s = \left(\frac{Sc}{Pr}\right)^{2/3} \left((H_{eff})(k)\left(\rho_a/\rho_w\right)^{0.5}(u_*)\right)^{-1} \quad (2)$$

where S_c = Schmidt number (unitless), Pr = Prandtl number (unitless), H_{eff} = dimensionless effective Henry's Law constant (ratio of aqueous to gas phase), k = von Karman constant (0.4), ρ_a = density of air (g cm^{-3}), ρ_w = density of water (g cm^{-3}) and u_* = friction velocity (m s^{-1}). The v_d value obtained using equations (1) and (2) is referred here as the standard deposition velocity and is used for most chemical species.

We revised the standard deposition velocity calculation to account for the enhanced deposition of O_3 due to the reaction with iodide in seawater. Similar to the work by Oh et al.[9], we implemented the approach of Chang et al.[5]. In this parameterization, R_S over seawater is calculated as:

$$R_s = \frac{1}{H_{eff}(ak_w+(\lambda D)^{1/2})} = \frac{1}{pk_w+q} \quad (3)$$

where k_w = gas transfer velocity (m s^{-1}), a = chemical enhancement factor, $(\lambda D)^{1/2}$ = chemical loss of O_3, $p = (a)(H_{eff}) = 1.75$, and $q = (\lambda D)^{1/2}(H_{eff})$. The values for k_w and q are calculated as:

$$k_w = \frac{k\left(\rho_a/\rho_w\right)^{0.5}(u_*)}{\left(\frac{S_c}{Pr}\right)^{2/3}} \quad (4)$$

$$q = [(k_i)(C_i)(d_w)]^{0.5}(H_{eff}) \quad (5)$$

where k_i is the second-order kinetic rate constant, C_i = concentrations of iodide in seawater [calculated using equation (9)], and d_w = diffusion coefficient of O_3 in water (m^2 s^{-1}). Magi et al.[51] reported a temperature dependent k_i ranging from 3.2×10^8 to 2.4×10^9 for a temperature range of 276-293 K that increases with increasing water temperature. We have used a constant value of 2.0×10^9 in our study[52]. Thus, our simulated impacts of enhanced O_3 deposition at lower water temperature will be somewhat greater than the real impacts. Similarly, simulated impacts of enhanced O_3 deposition at higher water temperature will be lower than the real impacts. The v_d value obtained using equations (1) and (3) is referred here as the enhanced deposition velocity.

Values of R_a and R_b are determined using the same procedures in standard and enhanced deposition velocity calculations.

CMAQ-derived standard O_3 deposition velocities over seawater are less than 0.01 cm s^{-1} while the enhanced O_3 deposition velocities generally range between 0.01-0.04 cm s^{-1} (Figure S.1). The median CMAQ-estimated standard and enhanced deposition velocities for O_3 over seawater are ~0.001 and 0.025 cm s^{-1}, respectively. Helmig et al.[4] reported median O_3 deposition velocities over different seawater ranging from 0.009 to 0.27 cm s^{-1}; therefore, the enhanced deposition velocities agree better with observations than the standard deposition velocities. However, further increases are needed for improving the agreement with observed deposition velocities.

2.3 Halogen chemistry

Several investigators have examined the role of bromine chemistry on O_3.[32-33, 36, 53] We use the Yang et al.[33] bromine chemistry with 5 additional reactions to account for the interactions of BrO with ClO and with DMS and BrO[32, 54]. A complete list of the bromine gas phase chemical reactions implemented in CMAQ can be found in Table S.1.

Numerous investigators have studied iodine chemistry[32, 34, 55], with Saiz-Lopez et al.[34] reporting a comprehensive mechanism of iodine gas phase chemical reactions, including photolysis of higher iodine oxides (I_2O_2, I_2O_3, and I_2O_4), listed in Table S.2. While previous studies[56-57] suggested that higher iodine oxides impact aerosol formation, Saiz-Lopez et al.[34] found that they also play a role in atmospheric chemistry and included their photochemical reactions in a global model. The Saiz-Lopez et al. study included two sets of iodine chemistry: one set without the

photolysis of I_2O_2, I_2O_3, and I_2O_4 (lower limit) and the other set with the photolysis of I_2O_2, I_2O_3, and I_2O_4 (upper limit). We completed two different model simulations with the halogen chemistry similar to that of Saiz-Lopez et al.[34] without and with the photochemical reactions of higher iodine oxides.

Yang et al.[33] considered heterogeneous hydrolysis of bromine nitrate ($BrONO_2$) on aerosols, which we also use (R1). We calculate the heterogeneous reaction rate of $BrONO_2$ using $k_{BrONO_2} = \frac{\gamma\, c\, A}{4}$, where γ = reactive uptake coefficient, c = mean molecular speed (m s^{-1}) (a function of temperature), and A = aerosol surface area (m^2 m^{-3}). Consistent with Yang et al.[33], we used $\gamma = 0.3$ following the recommendation of the International Union of Pure and Applied Chemistry (IUPAC). The recent IUPAC[58] evaluation provides values of 0.15-1.0 for the uptake coefficient of $BrONO_2$ on liquid substrates.

$$BrONO_2(g) + H_2O(aq) \rightarrow HOBr(g) + HNO_3(g) \quad \text{(R1)}$$

2.4 Halogen emissions

Marine emissions of bromine- and iodine-containing compounds fall into three categories with distinct formation mechanisms: 1) halocarbons, 2) inorganic bromine, and 3) inorganic iodine. Halocarbons are produced in the ocean by phytoplankton and macroalgae and typically have elevated oceanic concentrations in regions of high biological activity.[59] Halocarbon emissions are adapted from the Community Atmosphere Model with Chemistry (CAM-Chem)[35] and the Comprehensive Air quality Model with extensions (CAMx).[60] The halocarbons include five bromocarbons ($CHBr_3$, CH_2Br_2, CH_2BrCl, $CHBrCl_2$, $CHBr_2Cl$) and four iodocarbons (CH_3I,

231 CH_2ICl, CH_2IBr, CH_2I_2) and their emissions are estimated using monthly-average climatological
232 chl-*a* concentrations derived from the Moderate Resolution Imaging Spectroradiometer
233 (MODIS) aboard the Aqua satellite (oceancolor.gsfc.nasa.gov/cgi/l3) and projected to the polar
234 stereographic coordinate system used in the hemispheric CMAQ model. For each halocarbon, the
235 emission rate is calculated as:

236 $$E_{HC} = (O_F+S_F) \times A_{GC} \times 1.2\times10^{-11} \times f_{HC} \times f_{DP} \times \text{chl-}a \quad (6)$$

237 where E_{HC} = halocarbon emission rate (moles s^{-1}), O_F = open ocean zone fraction of the grid cell,
238 S_F = surf zone fractions of the grid cell, A_{GC} = grid cell area (m^2), 1.2×10^{-11} represents a base
239 emission rate, f_{HC} = a species-dependent emission factor, and f_{DP} = a diurnal profile factor based
240 on the grid cell local hour peaking at noon. Values of f_{HC} and f_{DP} from CAMx[60] are used.
241
242 Unlike halocarbons, which are directly emitted from the ocean surface, SSA are the source of the
243 one inorganic bromine compound (Br_2).[33] Bromine depletion in SSA is acidity dependent and
244 thought to be due to the uptake of gaseous HOBr[61] or HOCl[62] from the heterogeneous reaction of
245 N_2O_5 on aerosol surfaces. We use the simplified treatment of bromine release from SSA[33] as:

246 $$P_{SSA} = (O_F+S_F) \times A_{GC} \times 0.965\times10^{-16} \times U_{10}^{3.41} \times (0.38+0.054\times SSTC) \times \rho_{SSA} \quad (7)$$

247 $$E_{Br2} = 0.8624 \times P_{SSA} \times R_a \times DF / MW_{Br2} \quad (8)$$

248 where P_{SSA} = mass production of SSA with dry radius <10 μm (g s^{-1}), 0.965×10^{-16} represents
249 total volume flux of SSA at a wind speed of 1 m s^{-1} and relative humidity of 0%, U_{10} = 10-meter
250 wind speed (m s^{-1}), SSTC is the sea surface temperature in °C, ρ_{SSA} = dry SSA density (2.165 ×
251 10^3 g m^{-3}), E_{Br2} = Br_2 emission rate (moles s^{-1}), R_a = sea-salt Br/NaCl mass ratio (0.00223 g g^{-1}),
252 DF = bromine depletion factor (0.5), and MW_{Br2} = molecular weight of Br_2. In CMAQ, NaCl

represents 86.24% of the SSA emissions; thus we use a factor of 0.8624 to calculate NaCl emissions. Spatially, Br_2 emissions are consistent with the distribution of SSA emissions, which are positively related to U_{10} and SST in CMAQ as recently implemented by Gant et al.[63]

Mahajan et al.[64] compared model predictions to observed halogen species over the Atlantic Ocean and reported that current iodine fluxes are inadequate to explain the observed IO levels and additional iodine sources are needed. McDonald et al.[11] developed a parameterization for estimating emissions of two inorganic iodine species (HOI and I_2) based on the surface mixing ratios of O_3 in the atmosphere, iodide concentration at the sea surface, and wind speed. This parameterization is based on the production of HOI and I_2 from the reaction of iodide and O_3 in the interfacial layer of the ocean surface.[18] Following the global analysis from Chance et al.[10], we follow the MacDonald et al.[11] approach to estimate I_2 and HOI emissions that are driven by sea surface iodide concentrations ($[I^-_{(aq)}]$) based on SST:

$$[I^-_{(aq)}] = 1.46\times10^6 \times \exp\left(\frac{-9134}{SST}\right) \quad (9)$$

$$E_{I_2} = (O_F+S_F) \times A_{GC} \times 1.16\times10^{-14} \times [O_3] \times \left(4.15\times10^5 \times \left(\frac{\sqrt{[I^-_{(aq)}]}}{ws}\right) - \left(\frac{20.6}{ws}\right) - 23600 \times \sqrt{[I^-_{(aq)}]}\right) \quad (10)$$

$$E_{HOI} = (O_F+S_F) \times A_{GC} \times 1.16\times10^{-14} \times [O_3] \times [I^-_{(aq)}]^{1.3} \times \left(1.74\times10^9 - \left(6.54\times10^8 \times \ln ws\right)\right) \quad (11)$$

where E_{HOI} = HOI emission rates (mole s^{-1}), E_{I2} = I_2 emission rates (mole s^{-1}), $[O_3]$ = surface O_3 mixing ratios (ppbv), and ws = wind speed (m s^{-1}). We also set a lower limit of 3 m s^{-1} for wind speed following McDonald et al.[11].

Hemispheric halocarbons and inorganic halogen emissions estimates are shown in Table 1. Global halocarbon emissions can be calculated using publicly available global chl-*a* data. Using such data, we calculated global halocarbon emissions and compared to the values reported by others. Our global halocarbon emissions estimates compare well with values reported by Ordóñez et al.[32] Calculation of global inorganic halogen emissions requires global wind speed, SST, and O_3 fields. Since our modeling domain only covers the Northern Hemisphere, we could not accurately estimate global emissions of Br_2, HOI, and I_2. Our extrapolated global Br_2 emissions estimate is likely to be greater than the estimate of Parrella et al.[36] but is similar to the higher estimate of Yang et al.[33]. Our estimate accounts for the temperature effect on SSA; hence our Br_2 estimates extrapolated from the Northern Hemisphere during summertime conditions will be higher than those estimated without considering the temperature effect. Our Br_2 estimates are within the uncertainty factor of 4.0 for SSA sources.[65]

Prados-Roman et al.[66] implemented the McDonald et al.[11] parameterization into the CAM-Chem model and reported an annual global inorganic iodine emissions estimate of ~1,900 Gg (I). Our extrapolated global inorganic iodine emissions are likely to be greater than this value due to different O_3, SST, wind-speed fields. CMAQ predicted surface O_3 mixing ratios are higher than those predicted by CAM-Chem. The surface layer height in CMAQ is ~20 meters and we use wind-speeds at 10-m for calculating inorganic iodine emissions. In contrast, the surface layer height in CAM-Chem is ~150 meter and Prados-Roman et al.[66] used CAM-Chem model first layer wind-speeds for calculating these emissions. Differences in O_3 and wind-speed lead to greater iodine emissions in CMAQ. Additionally, we focus on summer-time when halogen emissions are likely to be greater than those in the winter-time. Similar to the Prados-Roman et

al.[66] estimates, our calculation also suggests that 95% of the inorganic iodine emissions are in the form of HOI and 5% are in the form of I_2.

Table 1: Halogen emissions estimates

Species	Hemispheric summer estimates in this study (Gg)	Global annual estimates in this study (Gg)	Global annual estimates from published studies (Gg)
$CHBr_3$	100.1	525	533
CH_2Br_2	17.2	90	67.3
CH_2BrCl	2.0	11	10.0
$CHBr_2Cl$	4.9	26	19.7
$CHBrCl_2$	4.8	17	22.6
CH_3I	44.9	236	303
CH_2ICl	49.2	258	234
CH_2IBr	18.3	96	87.3
CH_2I_2	24.4	128	116
Br_2	274 (Br)		1,150-2,090 (Br) 1,420 (Br)
HOI+ $2xI_2$	736 (I)		1,900 (I)

Note: Global annual estimates of halocarbon emissions are taken from Ordóñez et al.[32], global annual estimates of Br_2 are taken from Yang et al.[33] and Parrella et al.[36], and global annual estimates of HOI+$2\times I_2$ are taken from Saiz-Lopez et al.[34].

2.5 Simulation details

Four different model simulations were conducted. The first simulation (Case A) was completed using the standard O_3 deposition velocity over seawater and the CB05TUCl mechanism. The second simulation (Case B) was completed using the enhanced O_3 deposition over seawater and the CB05TUCl mechanism. The third simulation (Case C) was completed using the enhanced O_3 deposition over seawater, the CB05TUCl mechanism, and halogen chemistry without the photolysis of higher iodine oxides. The fourth simulation (Case D) was completed using the enhanced O_3 deposition over seawater, the CB05TUCl mechanism, and halogen chemistry with the photolysis of higher iodine oxides. Differences between Cases A and B are attributable to the enhanced deposition over seawater. Differences between Cases B and C simulation results are attributable to halogen chemistry without the photolysis of higher iodine oxides while the differences between Cases B and D are attributable to halogen chemistry with the photolysis of

higher iodine oxides. Each simulation was completed for four months (May-August) in 2006. May was used as model spin-up period and results of the three summer months (June-August) are analyzed.

3.0 RESULTS AND DISCUSSSION

3.1 Distribution of halogen species

The predicted mean surface mixing ratios for all halogen species over marine regions for Case C are presented in Table 2. HBr, produced via reactions of Br with HO_2 and aldehydes, contributes the highest percentage of total bromine. $CHBr_3$ is the second most abundant bromine species due to large emissions and a relatively long atmospheric lifetime. Br_2 is an emitted species but can also be formed in the atmosphere and is the third most abundant bromine species. CH_2Br_2 is an emitted species which only reacts with OH and is the fourth most abundant species. The fifth most abundant species is HOBr which is produced only by chemical reactions.

Table 2: Predicted mean surface mixing ratios of halogen species (Case C)

Species	Mean mixing ratio(pptv)	Percent distribution (%)	Species	Mean mixing ratio(pptv)	Percent distribution (%)
HBr	6.8	33.6	I_2O_3	5.0	58.6
$CHBr_3$	2.2	32.6	HOI	2.5	14.6
Br_2	1.3	13.1	CH_3I	2.1	12.2
CH_2Br_2	0.9	8.7	$IONO_2$	0.8	5.0
HOBr	1.3	6.4	IO	0.6	3.7
$CHBr_2Cl$	0.2	1.8	CH_2ICl	0.3	1.9
$BrONO_2$	0.2	1.1	I	0.2	0.9
BrO	0.2	0.8	I_2	0.1	0.7
$CHBrCl_2$	0.1	0.7	INO_2	0.1	0.6
CH_2BrCl	0.1	0.7	HI	0.1	0.6
CH_2IBr	0.1	0.3	CH_2I_2	<0.1	0.5
$BrNO_2$	<0.1	0.2	CH_2IBr	0.1	0.4
Br	<0.1	<0.1	OIO	<0.1	0.3
BrCl	<0.1	<0.1	I_2O_2	<0.1	<0.1
Total Br	20.2		INO	<0.1	<0.1
			I_2O_4	<0.1	<0.1
			ICl	<0.1	<0.1
			Total I	17.1	

Note: Total Br and Total I are calculated as follows:

Total Br = $3xCHBr_3 + HBr + 2xBr_2 + 2xCH_2Br_2 + HOBr + BrONO_2 + 2xCHBr_2Cl + BrO + CH_2BrCl + CHBrCl_2 + CH_2IBr + BrNO_2 + Br + BrCl$

Total I = $2xI_2O_2 + 2xI_2O_3 + 2x\ I_2O_4 + HOI + CH_3I + IONO_2 + IO + CH_2ICl + I + 2xI_2 + INO_2 + HI + 2xCH_2I_2 + CH_2IBr + OIO + INO + ICl$

The most abundant iodine species, I_2O_3, is a reaction product which does not participate in any other chemical reactions. The I_2O_3 mixing ratio decreases only via dry and wet deposition; enabling it to accumulate in the atmosphere. HOI is the second most abundant iodine species and is formed through primary emissions and secondary formation. CH_3I is the third most abundant iodine species due to its large emission rates and long atmospheric lifetime. $IONO_2$ is the fourth highest abundant iodine species.

Predicted surface BrO and IO mixing ratios (daytime mean over marine regions) are 0.3 pptv and 1.2 pptv, respectively. Since the rate constants for the reactions of Br + O_3 and I + O_3 are similar; the higher IO value relative to BrO suggests that the iodine chemistry is more effective in reducing O_3 than bromine chemistry. Saiz-Lopez et al.[35] compiled BrO and IO data from ground and ship-based measurements. Ground based measured BrO ranged 0.5-2.0 pptv and ship-based BrO ranged 3.0-3.6 pptv while ground based IO ranged 0.2-2.4 pptv and ship-based IO level was ~3.5 pptv. Prados-Roman et al.[19] reported IO measurements of 0.4-1.0 pptv in the global marine boundary layer. Mahajan et al.[64] reported a daytime average measurement of 2.8 pptv for BrO and 1.5 pptv for IO at Cape Verde in Atlantic Ocean. Thus, the halogen chemistry without the photolysis of higher iodine oxides successfully reproduces these observed halogen oxides. Higher levels (~100 pptv) of BrO have been measured in the boundary layer of the Dead Sea.[67-68] Our model results are lower than these high observed values over the Dead Sea which contains 86 times more bromide than typical ocean water.[69] Tas et al.[69] studied the atmospheric bromine chemistry over the Dead Sea using a one-dimensional model and reported that high levels of bromide in the Dead Sea water and release of halogen species from airborne aerosols are not

adequate to capture the observed BrO values. In their study, the addition of two heterogeneous reactions significantly improved the BrO predictions: the $BrONO_2$ heterogeneous reaction and the bromine explosion reaction. Our model uses typical ocean-water bromide levels and does not use the bromine explosion reaction. While our model uses the $BrONO_2$ heterogeneous reaction, the uptake coefficient is 2.5 times lower than the value used in their study. These differences likely caused our model predictions of BrO to be lower than high observed data over the Dead Sea.

3.2 Impact of enhanced O_3 deposition and halogen chemistry on O_3

Predicted mean O_3 averaged over all marine regions obtained with the standard deposition velocity is ~27 ppbv at surface and increases with altitude reaching ~330 ppbv at the highest model layer. The percent reductions due to the enhanced deposition and halogen chemistry are shown in Figure 1. The impact of the enhanced deposition is the highest at the surface (~3%), sharply decreases with height, and is expectedly negligible at higher altitudes. Though the impact of the halogen chemistry is also the highest at the surface, decreasing with height, it can effectively reduce O_3 concentrations throughout the lower troposphere. While halogen chemistry without photolysis of higher iodine oxides reduces surface O_3 mixing ratios over marine regions by 15%, including the photolysis of these oxides results in a more substantial decrease in surface O_3 mixing ratios averaging nearly 48%. As noted in section 3.1, I_2O_3 is the most abundant iodine species and the inclusion of its photolytic reaction reduces I_2O_3 mixing ratios and generates iodine which participates in O_3 destruction.

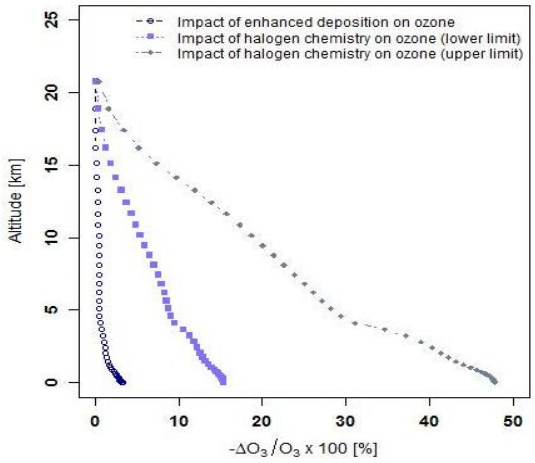

376
377 Figure 1: Percent reduction of O_3 due the enhanced deposition and halogen chemistry
378

379 The spatial distributions of summertime mean surface O_3 mixing ratios predicted by Case A and
380 reduction due to enhanced deposition velocity and halogen chemistry are presented in Figure 2.
381 Higher O_3 mixing ratios are predicted over terrestrial and coastal areas than over remote marine
382 regions. Enhanced deposition reduces O_3 mixing ratios by 1.0-2.0 ppbv over most marine regions
383 and by 2.0-3.0 ppbv over some coastal regions. The impact of the enhanced deposition in remote
384 marine areas is relatively small due to lower absolute mixing ratios. Halogen chemistry without
385 photolysis of higher iodine oxides reduces O_3 mixing ratios in the majority of the modeling
386 domain. However, the reduction is greater over the marine environment than over land. O_3
387 mixing ratios are reduced by 4.0-6.0 ppbv over most remote marine regions and over 6.0 ppbv
388 occurs in several coastal areas. Over most terrestrial regions near the coast, O_3 mixing ratios are
389 reduced by 2.0-4.0 ppbv due to halogen chemistry. The inclusion of the photochemical reactions
390 of higher iodine oxides has a large impact on predicted O_3 mixing ratios, with reductions of 12-
391 24 ppbv over large swaths of the marine domain.
392
393 Yang et al.[33] reported that bromine chemistry reduces 4-6% of monthly mean summertime
394 tropospheric O_3 in Northern Hemisphere while Parrella et al.[36] reported a global tropospheric O_3

reduction of 6.5% due to the bromine chemistry. Saiz-Lopez et al.[34] reported that iodine chemistry reduces annual mean tropical tropospheric O_3 by 9% and 16% for the simulations without and with photolysis of higher iodine oxides, respectively. Saiz-Lopez et al.[35] reported tropical tropospheric O_3 loss of 6-20% due to combined bromine and iodine chemistry. The halogen chemistry mediated O_3 reductions in this study are greater than those reported by others due to bromine chemistry or iodine chemistry alone but similar to values reported by others studying the combined effects of bromine and iodine chemistry. The reduction of O_3 mixing ratios due to halogen chemistry with photolysis of higher iodine species in this study is greater than values reported by other investigators.

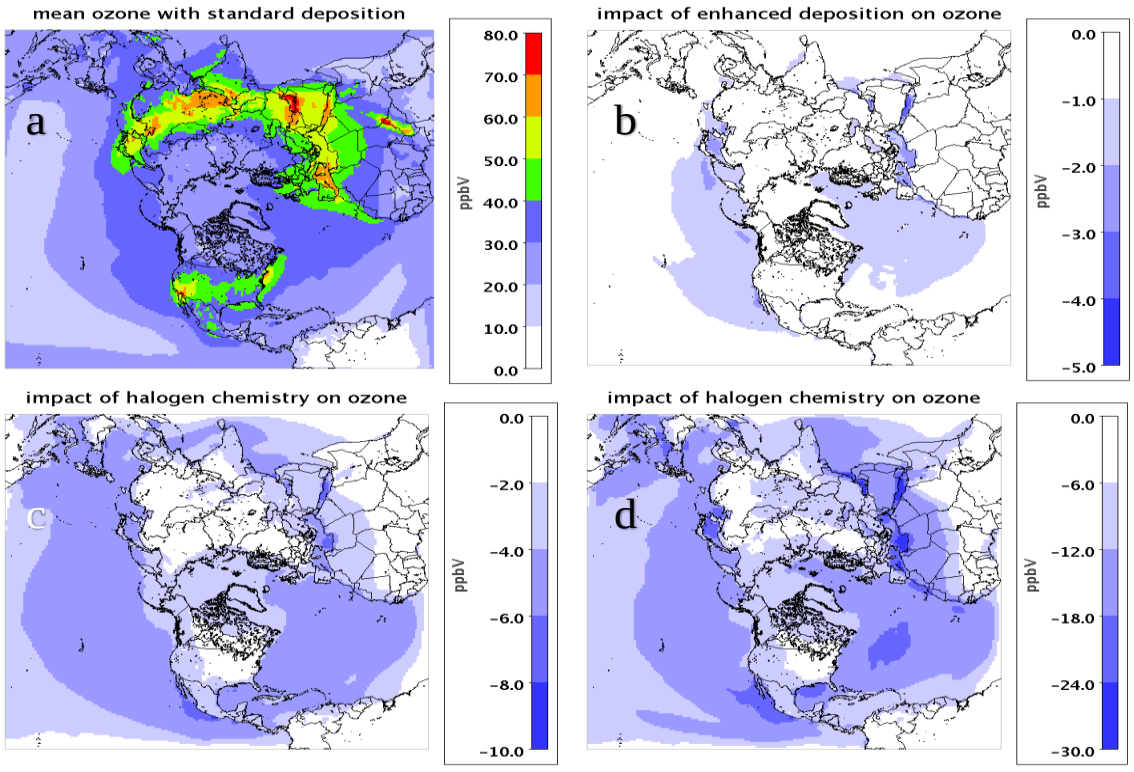

Figure 2: (a) Spatial distribution of predicted mean summertime O_3 with the standard deposition (b) reduction of O_3 due to enhanced deposition (c) reduction of O_3 due to the halogen chemistry without photolysis of higher iodine oxides (d) reduction of O_3 due to the halogen chemistry with photolysis of higher iodine oxides

3.3 Impact of halogen chemistry on selected chemical species

Mahajan et al.[64] compared model predictions to observed data from Cape Verde and reported a typical observed peak noon value of 0.25 pptv for OH, 18 pptv for HO_2, and 72 for HO_2:OH ratio. They found that their baseline model simulation under-predicts OH by ~13%, over-predicts HO_2 by ~14%, and over-predicts HO_2:OH compared to observations, but improves with the inclusion of halogen chemistry. The inclusion of the halogen chemistry in our simulations decreased mean OH by 1% and HO_2 by 11%, and lowered the HO_2:OH from 104 to 93 over marine regions. Though we cannot directly compare our predictions to observations, our results qualitatively agree with those reported by Mahajan et al.[64] Several halogen compounds react with HO_2, reducing both its mixing ratio and the mixing ratio of H_2O_2 (by 17%) over marine regions. Because H_2O_2 and O_3 are important oxidizing agents for aqueous-phase conversion of SO_2 into sulfate, the production of sulfate via the aqueous-phase oxidation by H_2O_2 and O_3 decreases with the inclusion of halogen chemistry.

3.4 Comparison with observed data

Model predictions are compared to the observed data at selected monitoring sites from the World Data Centre for Greenhouse Gases (http://ds.data.jma.go.jp/gmd/wdcgg). Since a relatively coarse horizontal grid-size is used in this study, we limit our comparisons to 13 background sites (Table S.3) where enhanced deposition and halogen chemistry are effective in reducing O_3. The median observed O_3 for these sites is 27 ppbv (Figure 3), which is over-predicted by ~6 ppbv in Case A. The simulation with enhanced deposition (Case B) improves model performance by lowering the median prediction by ~1 ppbv. The simulation including halogen chemistry without photolysis of higher iodine oxides (Case C) further reduces the surface O_3 mixing ratios by 5 ppbv. Case D, which uses halogen chemistry with photolysis of higher iodine oxides, has a more

substantial reduction of surface O_3 mixing ratios averaging 12 ppbv compared to that of Case B. The inclusion of enhanced deposition and halogen chemistry without photolysis of higher iodine oxides improve model performance. When the photolysis reactions are included in Case D, the surface O_3 mixing ratios are under-predicted by the model. This evaluation suggests that additional research is needed to further refine the halogen emissions and chemistry.

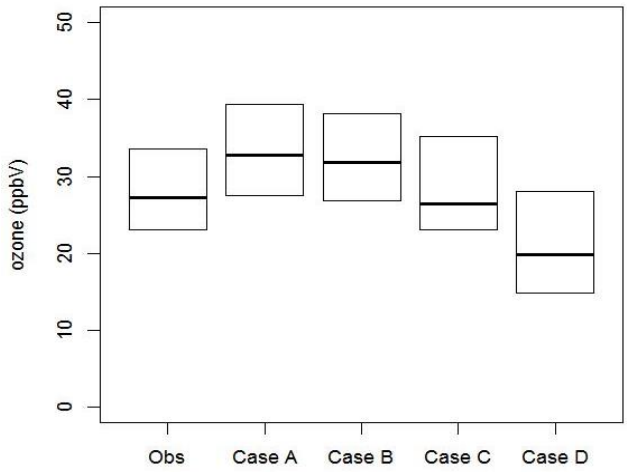

Figure 3: A comparison of model predictions with observed data. Lower bar in the box represents 25th percentile, middle bar represents the median and the upper bar represents 75 percentile values.

3.5 An effective first order rate constant for halogen mediated O_3 loss

The application of regional air quality models demands computational efficiency. Because the inclusion of detailed halogen chemistry increases computational time (in our case by more than 25%), simplifications such as the first order rate constant can be used for calculating halogen mediated O_3 loss in these computationally intensive model applications. The following relationship between the first order rate constant values, k_{O3} (s^{-1}), and the atmospheric pressures, P (Pa) is obtained using nonlinear least squares estimation ($R^2 = 0.97$) (Figure S.2).

$$k_{O3}(P) = 1.0000 \times 10^{-40} e^{7.7400 \times 10^{-4} \times P} + 4.0582 \times 10^{-09} e^{5.7451 \times 10^{-5} \times P} \quad (12)$$

3.6 Future work

We examined the impacts of enhanced O_3 deposition and halogen chemistry on summertime O_3. Future work is needed to quantify the impact of these processes during other seasons. Our enhanced deposition scheme neglects several factors such as the possible reaction of dimethyl sulfide[5] and dissolved organic carbon[7] with O_3 as well as the effects of water salinity[70] and surface properties[8]. Our study uses a simplified Br_2 emission scheme which may contain large uncertainties. Studies suggest that heterogeneous reactions involving marine aerosols and O_3 can release bromine and iodine.[24, 25, 27] Our study does not include the bromine explosion reaction[69] that may occur in some marine boundary layers. While we have attempted to include the most important atmospheric bromine and iodine reactions, it is possible that other reactions not included in this study may also affect model results. Photochemical reactions of higher iodine oxides in the halogen chemistry treatment contain large uncertainties. Thus, future effort should focus on reducing these uncertainties and re-examining the impacts with improved enhanced deposition scheme and halogen chemistry. Previous studies employing regional air quality models have shown over-predictions of O_3 in coastal areas[71-73] and may need to be reexamined with a more realistic representation of enhanced O_3 deposition and halogen chemistry as presented in this study. Some of these studies also have revealed that lateral boundary conditions used in regional models play an important role in O_3 predictions; this suggests that future studies focusing on O_3 predictions in coastal areas should use boundary conditions generated from hemispheric or global models which include enhanced O_3 deposition and halogen chemistry.

DISCLAIMER

Although this paper has been reviewed by EPA and approved for publication, it does not necessarily reflect EPA's policies or views.

REFERENCES

1. Devlin, R.; Folinsbee, L.; Biscardi, F.; Hatch, G.; Becker, S.; Madden, M.; Robbins, M.; Koren, H. Inflammation and cell damage induced by repeated exposure of humans to ozone. Inhalation Toxicology, 1997, 9:211–235.
2. Felzer, B.S.; Cronin, T., Reilly, J. M.; Melillo, J. M.; Wang, X. Impacts of ozone on trees and crops. C.R. Geoscience, 2007, 339:784-798.
3. Gallagher, M. W.; Beswick, K. M.; McFiggans, G.; Coe, H., Choularton, T. W. Ozone dry deposition velocities for coastal waters. Water, Air, & Soil Pollution, 2001, 1, 233–242.
4. Helmig, D.; Lang, E. K.; Bariteau, L.; Boylan, P.; Fairwall, C. W., Ganzeveld, L.; Hara, J. E.; Hueber, J.; Pallandt, M. Atmosphere-ocean ozone fluxes during the TexAQS 2006, STRATUS 2006, GOMECC 2007, GasEx 2008, and AMMA 2008 cruises. Journal of Geophysical Research, 2012, 117, D04305.
5. Chang, W.; Heikes, B. G.; Lee, M. Ozone deposition to the sea surface: chemical enhancement and wind speed dependence. Atmospheric Environment, 2004, 38, 1053–1059.
6. Ganzeveld, L.; Helmig, D.; Fairall, C. W.; Hare, J.; Pozzer, A. Atmosphere-ocean ozone exchange - a global modeling study of biogeochemical, atmospheric and water-side turbulence dependencies. Global Biogeochemical Cycle, 2009, 23, GB4021.
7. Shaw, M.D.; Carpenter, L.J. Modification of ozone deposition and I_2 emissions at the air-aqueous interface by dissolved organic carbon of marine origin. Environmental Science & Technology, 2013, 47, 10947-10954.
8. Resser, D.I.; Donaldson, D. J. Influence of water surface properties on the heterogeneous reaction between $O_{3(g)}$ and $I^-_{(aq)}$. Atmospheric Environment, 2011, 45, 6116-6120.
9. Oh, I.-B.; Byun, D. W.; Kim, H.-C.; Kim, S.; Cameron, B. Modeling the effect of iodide distribution on ozone deposition to seawater surface. Atmospheric Environment, 2008, 42, 4453–4466.
10. Chance, R.; Baker, A. R.; Carpenter, L.; Jickells, T. D. The distribution of iodide at the sea surface. Environmental Science: Processes and Impacts, 2014, 16, 1841–1859.
11. MacDonald S. M.; Martin, J.C.G.; Chance, R., Warriner, S.; Saiz-Lopez, A.; Carpenter, LJ, Plane JMC. A laboratory characterisation of inorganic iodine emissions from the sea surface: dependence on oceanic variables and parameterisation for global modelling. Atmospheric Chemistry & Physics, 2014, 14, 5841-5852.
12. Fairall, C.W.; Helmig, D.; Ganzeveld, L.; Hare, J. Water-side turbulence enhancement of ozone deposition to the ocean. Atmospheric Chemistry & Physics, 2007, 7, 443-451.
13. Peters, C.; Pechtl, S.; Stutz, J.; Hebestreit, K.; Hönninger, G.; Heumann, K. G.; Schwarz, A.; Winterlik, J.; and Platt, U. Reactive and organic halogen species in three different European coastal environments. Atmospheric Chemistry & Physics, 2005, 5, 3357-3375, doi:10.5194/acp-5-3357-2005.
14. Mahajan, A.S.; Oetjen, H.; Saiz-Lopez, A.; Lee, J.D.; McFiggans, G.B.; Plan, J.M.C. Reactive iodine species in a semi-polluted environment. Geophysical Research Letters, 36, 2009, L16803, doi:10.1029/2009GL038018.
15. Simpson, W. R.; Brown, S. S.; Saiz-Lopez, A.; Thornton, J.A.; Von Glasow, R. Tropospheric Halogen Chemistry: Sources, Cycling, and Impacts. Chemical Reviews, 2015, 115, 4035-4062, doi:10.1021/cr5006638.
16. Alicke, B.; Hebestreit, K.; Stutz, J.; Platt, U. Iodine oxide in the marine boundary layer. Nature, 1999, 397, 572–573.
17. Read, K. A.; Mahajan, A. S.; Carpenter, L. J.; Evans, M. J.; Faria, B. V. E.; Heard, D. E.; Hopkins, J. R.; Lee, J. D.; Moller, S. J.; Lewis, A. C.; Mendes, L.; McQuaid, J. B.; Oetjen, H.; SaizLopez, A.; Pilling, M. J.; Plane, J. M. C. Extensive halogen mediated ozone destruction over the tropical Atlantic Ocean. Nature, 2008, 453, 1232–1235.
18. Carpenter, L. J.; MacDonald, S. M.; Shaw, M. D.; Kumar, R.; Saunders, R. W.; Parthipan, R.; Wilson, J.; Plane, J. M. C. Atmospheric iodine levels influenced by sea surface emissions of inorganic iodine. Nature Geoscience, 2013, 6, 108–111.
19. Prados-Roman, C.; Cuevas, C. A.; Hay, T.; Fernandez, R. P.; Mahajan, A.S.; Royer, S.-J.; Gali, M.; Simo, R.; Dachs, J.; Gro□mann, K.; Kinnison, D. E.; Lamarque, J-F.; Saiz-Lopez, A. Iodine oxide in the global marine boundary layer. Atmospheric Chemistry & Physics, 2015, 15, 583-593.
20. Mahajan, A. S., Gómez Martín, J. C., Hay, T. D., Royer, S.-J.,Yvon-Lewis, S., Liu, Y., Hu, L., Prados-Roman, C., Ordóñez, C., Plane, J. M. C., and Saiz-Lopez, A. Latitudinal distribution of reactive iodine in the Eastern Pacific and its link to open ocean sources. Atmospheric Chemistry & Physics, 2012, 12, 11609–11617, doi:10.5194/acp-12-11609-2012.
21. O'Dowd, C.; Jimenez, J.; Bahreini, R.; Flagan, R.; Seinfeld, J.; Hameri, K.; Pirjola, L.; Kulmala, M.; Jennigns, S.; Hoffmann, T. Marine aerosol formation from biogenic iodine emissions. Nature, 2002, 417, 632–636.
22. Holmes, C. D.; Jacob, D. J.; Corbitt, E. S.; Mao, J.; Yang, X.; Talbot, R.; Slemr, F. Global atmospheric model for mercury including oxidation by bromine atoms. Atmospheric Chemistry & Physics, 2010, 10, 12037–12057.

23. Saiz-Lopez, A. and von Glasow, R. Reactive halogen chemistry in the troposphere. Chemical Society Reviews, 2012, 41, 6448–6472.
24. Hunt, S. W.; Roeselova´, M.; Wang, W.; Wingen, L.M.; Knipping, E.M.; Tobias, D.J.; Dabdub, D.; Finlayson-Pitts, B. J. Formation of molecular bromine from the reaction of ozone with deliquesced NaBr aerosol: evidence for interface chemistry. The Journal of Physical Chemistry A, 2004, 108, 11559-11572.
25. Clifford, C.; Donaldson, D. J. Direct experimental evidence for a heterogeneous reaction of ozone with bromide at the air-aqueous interface. The Journal of Physical Chemistry A, 2007, 111, 9809-9814.
26. Rouvière, A.; Ammann, M. The effect of fatty acid surfactants on the uptake of ozone to aqueous halogenide particles. Atmospheric Chemistry & Physics, 2010, 10, 11489-11500.
27. Pillar, E.A.; Guzman, M.I.; Rodruguez, J.M. Conversion of iodide to hypoiodous acid and iodine in aqueous microdroplets exposed to ozone. Environmental Science & Technology, 2013, 47, 10971-10979.
28. Lee, M-T.; Brown, MA; Kato S.; Kleibert A.; Türler, A.; Ammann, M. Competition between organics and bromide at the aqueous solution−air interface as seen from ozone uptake kinetics and x‑ray photoelectron spectroscopy. The Journal of Physical Chemistry A, 2015, 119, 4600-4608.
29. vonGlasow, R.; Sander, R.; Bott, A.; Crutzen, P. J. Modeling halogen chemistry in the marine boundary layer. 1. Cloud-free MBL. Journal of Geophysical Research, 2002, 107, 4341.
30. Von Glasow, R.; Sander, R.; Bott, A.; Crutzen, P. J. Modeling halogen chemistry in the marine boundary layer. 2. Interactions with sulfur and cloud-covered MBL. Journal of Geophysical Research, 2002, 107, 4323.
31. Warwick, N. J.; Pyle, J. A.; Carver, G. D.; Yang, X.; Savage, N. H.; O'Connor, F. M.; and Cox, R. A. Global modeling of biogenic bromocarbons, Journal of Geophysical Research, 2006, 111, D24305.
32. Ordóñez, C.; Lamarque, J.-F.; Tilmes, S.; Kinnison, D. E.; Atlas, E. L.; Blake, D. R.; Sousa Santos, G.; Brasseur, G.; Saiz-Lopez, A. Bromine and iodine chemistry in a global chemistry-climate model: description and evaluation of very short-lived oceanic sources. Atmospheric Chemistry & Physics, 2012, 12, 1423-1447.
33. Yang, X.; Cox, R. A.; Warwick, N. J.; Pyle, J. A.; Carver, G. D.; O'Connor, F. M.; Savage, N. H. Tropospheric bromine chemistry and its impacts on ozone: A model study. Journal of Geophysical Research, 2005, 110, D23311.
34. Saiz-Lopez, A.; Fernandez, R. P.; Ordóñez, C.; Kinnison, D. E.; Gómez Martín, J. C.; Lamarque, J.-F.; Tilmes, S. Iodine chemistry in the troposphere and its effect on ozone. Atmospheric Chemistry & Physics, 2014, 14, 13119-13143.
35. Saiz-Lopez, A.; Lamarque, J.-F.; Kinnison, D. E.; Tilmes, S.; Ordóñez, C.; Orlando, J. J.; Conley, A. J.; Plane, J. M. C.; Mahajan, A. S.; Sousa Santos, G., Atlas, E. L.; Blake, D. R., Sander, S. P.; Schauffler, S.; Thompson, A. M.; Brasseur, G. Estimating the climate significance of halogen-driven ozone loss in the tropical marine troposphere. Atmospheric Chemistry & Physics, 2012, 12, 3939–3949.
36. Parrella, J. P.; Jacob, D. J.; Liang, Q.; Zhang, Y.; Mickley, L. J.; Miller, B.; Evans, M. J.; Yang, X.; Pyle, J. A.; Theys, N.; Van Roozendael, M. Tropospheric bromine chemistry: implications for present and pre-industrial ozone and mercury. Atmospheric Chemistry & Physics, 2012, 12, 6723–6740.
37. Long, M. S.; Keene, W. C.; Easter, R. C.; Sander, R.; Liu, X.; Kerkweg, A.; Erickson, D. Sensitivity of tropospheric chemical composition to halogen-radical chemistry using a fully coupled size-resolved multiphase chemistry–global climate system: halogen distributions, aerosol composition, and sensitivity of climate-relevant gases. Atmospheric Chemistry & Physics, 2014, 14, 3397-3425
38. Rouvière, A.; Sosedova, Y.; Markus Ammann, M. Uptake of ozone to deliquesced KI and mixed KI/NaCl aerosol particles. The Journal of Physical Chemistry A, 2010, 114, 7085-7093.
39. Liu, Q.; Schurter, L.M.; Muller, C.E.; Aloisio, S.; Francisco, J.S.; Margerum, D.W. Kinetics and mechanisms of aqueous ozone reactions with bromide, sulfite, hydrogen sulfite, iodide, and nitrite ions. Inorg. Chem. 2001**,** 40, 4436-4442.
40. Byun, D.; Schere, K. L. Review of the governing equations, computational algorithms, and other components of the Models-3 Community Multiscale Air Quality (CMAQ) Modeling System. Applied Mechanics Reviews, 2006, 59, 51-77.
41. Foley K. M.; Roselle, S. J.; Appel, K. W.; Bhave, P. V.; Pleim, J. E.; Otte, T. L.; Mathur, R.; Sarwar, G.; Young, J. O.; Gilliam, R. C.; Nolte, C. G.; Kelly, J.; Gilliland, A.B.; Bash, J. O. Incremental Testing of the Community Multiscale Air Quality (CMAQ) Modeling System Version 4.7. Geoscientific Model Development, 2010, 3, 205-226.
42. Sarwar, G.; Simon, H.; Bhave, P.; Yarwood, G. Examining the impact of heterogeneous nitryl chloride production on air quality across the United States. Atmospheric Chemistry & Physics, 2012, 12, 1-19.

43. Appel, K.W.; Pouliot, G.; Simon, H.; Sarwar, G.; Pye, H.O.T.; Napelenok, S.; Akhtar, F.; Roselle, S.J. Evaluation of dust and trace metal estimates from the Community Multiscale Air Quality (CMAQ) model version 5.0. Geoscientific Model Development, 2013, 6, 883-899.
44. Sarwar, G.; Godowitch, J.; Henderson, B.H.; Fahey, K.; Pouliot, G.; Hutzell, W.T.; Mathur, R.; Kang, D.; Goliff, W.S.; Stockwell, W.R. A comparison of atmospheric composition using the Carbon Bond and Regional Atmospheric Chemistry Mechanisms. Atmospheric Chemistry and Physics, 2013, 13, 9695-9712.
45. Mathur, R.; Gilliam, R.; Bullock, O. R.; Roselle, S.; Pleim, J.; Wong, D.; Binkowski, F.; Streets, D. Extending the applicability of the community multiscale air quality model to hemispheric scales: motivation, challenges, and progress. In Air Pollution Modeling and its Applications XXI, Steyn, D. G., Trini, S., Eds.; The NATO Science for Peace and Security Programme, Springer, Dordrecht, The Netherlands, Chapter 30, 175–179, 2012.
46. Mathur, R.; Roselle, S.; Young, J.; Kang, D. Representing the effects of long-range transport and lateral boundary conditions in regional air pollution models. In Air Pollution Modeling and its Application XXII, Steyn, D. G., Builtjes, P.J.H., Timmermans, R.M.A., Eds.; The NATO Science for Peace and Security Programme, Springer, Heidelberg, Germany, Chapter 51, 303–308, 2014.
47. Sarwar, G.; Simon, H.; Xing, J.; Mathur, R. Importance of tropospheric $ClNO_2$ chemistry across the Northern Hemisphere. Geophysical Research Letters, 2014, 41, 4050-4058.
48. Xing, J.; Mathur, R.; Pleim, J.; Hogrefe, C.; Gan, C.-M.; Wong, D. C.; Wei, C.; Gilliam, R.; Pouliot, G. Observations and modeling of air quality trends over 1990–2010 across the Northern Hemisphere: China, the United States and Europe. Atmospheric Chemistry & Physics, 2015, 15, 2723-2747.
49. Wesley, M. L. Parameterization of surface resistances to gaseous dry deposition in regional scale numerical models. Atmospheric Environment, 1989, 23, 1293-1304.
50. Slinn, W. G. N.; Hasse, L.; Hicks, B.B.; Hogan, A.W.; Lal, D.; Liss, P.S.; Munnich, K.O.; Sehmel, G.A.; Vittori O. Some aspects of the transfer of atmospheric trace constituents past the air-sea interface. Atmospheric Environment, 1978, 12: 2055-2087.
51. Magi, L.; Schweitzer, F.; Pallares, C.; Cherif, S.; Mirabel, P.; George, C. Investigation of the uptake rate of ozone and methylhydroperoxide by water surfaces. The Journal of Physical Chemistry A, 1997, 101 (27), 4943−4949.
52. Garland, J. A.; Elzerman, A. W.; Penkett, S. A. The mechanism for dry deposition of ozone to seawater surfaces. Journal of Geophysical Research, 1980, 85 (12), 7488−7492.
53. Fernandez, R. P.; Salawitch, R. J.; Kinnison, D. E.; Lamarque, J.-F.; Saiz-Lopez, A. Bromine partitioning in the tropical tropopause layer: implications for stratospheric injection. Atmospheric Chemistry and Physics, 2014, 14, 13391-13410.
54. Sommariva, R.; Glasow, R. Multiphase Halogen Chemistry in the Tropical Atlantic Ocean. Environmental Science & Technology, 2012, 46 (19), 10429–10437.
55. Solomon, S.; Garcia, RR.; Ravishankara, A. R. On the role of iodine in ozone depletion. Journal of Geophysical Research, 1994, 99, D10, 20,491-20,499.
56. Hoffmann, T.; O'Dowd, C. D.; Seinfeld, J. H. Iodine oxide homogeneous nucleation: an explanation for coastal new particle production. Geophysical Research Letters, 2001, 28, No. 10, 1949-1952.
57. Burkholder, J. B.; Curtius, J.; Ravishankara, A. R.; Lovejoy, E. R. Laboratory studies of the homogeneous nucleation of iodine oxides. Atmospheric Chemistry & Physics, 2004, 4, 19-34.
58. Ammann, M., Cox, R. A., Crowley, J. N., Jenkin, M. E., Mellouki, A., Rossi, M. J., Troe, J., and Wallington, T. J.: Evaluated kinetic and photochemical data for atmospheric chemistry: Volume VI – heterogeneous reactions with liquid substrates, Atmos. Chem. Phys., 13, 8045–8228, 2013, IUPAC Task Group on Atmospheric Chemical Kinetic Data Evaluation, http://iupac.pole-ether.fr/index.html.
59. Liss, P. S.; Marandino, C.; Dahl, E. E.; Helmig, D.; Hintsa, E. J.; Hughes, C.; Johnson, M. T.; Moore, R. M.; Plane, J. M. C.; Quack, B.; Singh, H. B.; Stefels, J.; Glasow, R.; Williams, J. Short-Lived Trace Gases in the Surface Ocean and the Atmosphere Ocean-Atmosphere Interactions of Gases and Particles. Springer, Berlin, Germany, 1-54, doi:10.1007/978-3-642-25643-1_1, 2014.
60. Yarwood, G.; Jung, J; Ou, N.; Emery, C., 2012. Improving CAMx performance in simulating ozone transport from the Gulf of Mexico, Final Report for the Texas Commission on Environmental Quality, Project No. 0626408I.
61. Fan, S.-M.; Jacob, D. J. Surface ozone depletion in Arctic spring sustained by bromine reactions on aerosols. Nature, 1992, 359, 522–524.
62. Vogt, R.; Crutzen, P. J.; Sander, R. A mechanism for halogen release from sea-salt aerosol in the remote marine boundary layer. Nature, 1996, 383, 327–330.
63. Gantt, B., Kelly, J. T., and Bash, J. O. Updating sea spray aerosol emissions in the Community Multiscale Air Quality (CMAQ) model version 5.0.2. Geoscientific Model Development Discussions, 2015, 8, 3905-3939.

64. Mahajan, A. S.; Plane, J. M. C.; Oetjen, H.; Mendes, L.; Saunders, R. W.; Saiz-Lopez, A.; Jones, C. E.; Carpenter, L. J.; McFiggans, G. B. Measurement and modelling of tropospheric reactive halogen species over the tropical Atlantic Ocean. Atmospheric Chemistry & Physics, 2010, 10, 4611-4624.
65. Lewis, E.R.; Schwartz, S.E. Sea salt aerosol production: mechanisms, methods, measurements, and models – a critical review. Geophysical Monograph, 2004, 152, AGU, Washington, D. C.
66. Prados-Roman, C.; Cuevas, C. A.; Fernandez, R. P.; Kinnison, D. E.; Lamarque, J-F.; Saiz-Lopez, A. A negative feedback between anthropogenic ozone pollution and enhanced ocean emissions of iodine. Atmospheric Chemistry & Physics, 2015, 15, 2215-2224.
67. Matveev, V., Peleg, M., Rosen, D., Tov-Alper, D. S., Hebestreit, K., Stutz, J., Platt, U., Blake, D., Luria, M. Bromine-oxide-ozone interaction over the Dead Sea. Journal of Geophysical Research, 2001, 16, No., D10, 10,375-10,387.
68. Holla, R., Schmitt, S., Friess, U., PÃ¶hler, D., Zingler, J., Corsmeier, U., Platt, U., Vertical distribution of BrO in the boundary layer at the Dead Sea. Environmental Chemistry, EN14224, Accepted 27 March 2015.
69. Tas, E., Peleg, M., Pedersen, D. U., Matveev, V., Pour Biazar, A., and Luria, M. Measurement-based modeling of bromine chemistry in the boundary layer: 1. Bromine chemistry at the Dead Sea. Atmospheric Chemistry & Physics, 2006, 6, 5589-5604.
70. Colman, L.; Varghese, S.; Tripathi, O.P.; Jennings, S.G.; O'Dowd, C.D. Regional-scale ozone deposition to North-East Atlantic waters. Advances in Meteorology, 2010, 2010, Article ID 243701, 16 pages.
71. Eder, B. K.; Yu. S. A Performance evaluation of the 2004 release of Models-3 CMAQ. Atmospheric Environment, 2006, 40(26):4811-4824.
72. Han, Z.; Sakurai, T.; Ueda, H.; Carmichael; G. R.; Streets, D., Hayami, H., Wang, Z.; Holloway, T., Engardt, M., Hozumi, Y.; Park, S.U.; Kajino, M.; Sarttelet, K.; Fung, C.; Bennet, C.; Thongboonchoo, N.; Tang, Y.; Chang, A.; Matsuda, K.; Amman, M. MICS-Asia II: Model intercomparison and evaluation of ozone and relevant species. Atmospheric Environment, 2008, 42, 15:3491–3509.
73. Appel, W.; Chemel, C.; Roselle, S. J.; Francis, X. V., Rong-Ming, H.; Sokhi, R. S.; Rao, S. T.; Galmarini, S. Examination of the Community Multiscale Air Quality (CMAQ) Model Performance over the North American and European Domains. Atmospheric Environment, 2012, 53:142-155.